
Adaptive remeshing and error control for forming processes

Lionel Fourment — Jean-Loup Chenot

CEMEF

Ecole des Mines de Paris
rue Claude Daunesse, BP 207
06904 Sophia Antipolis cedex

ABSTRACT. In order to take into account the large deformations of the material, the numerical simulation of forming problems invokes a great number of meshings. For effective treatment of meshing and remeshing, error estimators have been considered as a guiding tool. The present work especially concerns methods for the construction of adapted meshes when an optimal size criterion has been calculated from error estimators. The remeshing procedure is based on the Delaunay type mesh generator and on the uncoupling between geometric and adaptivity constraints of the remeshing problem. The procedure is tested for various elasticity and viscoplasticity problems. It is shown to be robust and reliable, then it is used to compare the efficiency of two error indicators which stem from the Z_2 (Zienkiewicz and Zhu) error estimator and the Δ error estimators (a correction of the Z_2 estimate in order to take into account the unbalancing of the smoothed stress tensor) which have been suggested in a previous paper. Singular problems are tackled : iterations of the adaptive remeshing method makes it possible to solve them. This method is then used to control the discretization error during several non-steady complex forming problems.

RÉSUMÉ. La simulation numérique des procédés de mise en forme nécessite un très grand nombre de remaillages afin de prendre en compte les grandes déformations que subit le matériau. Les méthodes d'estimation d'erreur ont été proposées pour résoudre ce type de problème. Ce travail concerne plus particulièrement les méthodes de construction de maillages adaptés, lorsque le critère de taille optimale est le résultat de l'estimation d'erreur. La procédure de maillage utilisée repose sur un algorithme de type Delaunay et sur un traitement en deux temps des contraintes d'ordre géométrique et des contraintes d'ordre adaptatif. La procédure est testée sur plusieurs problèmes d'élasticité et de viscoplasticité, pour lesquels elle s'avère robuste et fiable. Elle est utilisée pour comparer l'efficacité de deux estimateurs d'erreur préalablement proposées pour la mise en forme : un estimateur de type Zienkiewicz et Zhu et un estimateur Δ , qui introduit une correction à l'estimateur précédent de manière à prendre en compte le non-respect des équations d'équilibre par le tenseur des contraintes lissé. Les problèmes avec singularités sont résolus par des itérations de la méthode de maillage adaptatif.

Cette méthode est enfin appliquée au contrôle de l'erreur de discrétisation au cours de la simulation de plusieurs procédés de mise en forme instationnaires.

KEY WORDS : error estimator, adaptive meshing, remeshing, Delaunay tessellation, viscoplasticity, non steady-state process, metal forming, forging, machining.

MOTS-CLÉS : estimateur d'erreur, maillage adaptatif, remaillage, triangulation de Delaunay, viscoplasticité, procédé instationnaire, mise en forme, forgeage, usinage.

1. Introduction

The numerical simulation of non-steady forming processes such as forging requires a great number of remeshing steps. Indeed, the deformations of the material are so important that they cannot be calculated with a single finite element mesh using a lagrangian formulation. For instance, the accurate simulation of forging processes usually requires about fifty remeshings [HAN92]. So it is obvious that the remeshing operations should be fully automatic, as well as robust and reliable. Error estimation and adaptive remeshing techniques have been developed to answer this question. The problem can be split into two parts : first, find an accurate estimation of the discretization error and then, build a mesh of a given accuracy.

Although error estimators have been especially studied for linear problems, some recent works are dedicated to forming processes : Hétu and Pelletier [HET92] in the field of both linear and viscous incompressible flows, Baranger and El Amri [BAR89] for quasi-newtonian flows, Zienkiewicz, Liu and Huang [ZIE88], Fourment and Chenot [FOU94] for viscoplastic materials, Ladevèze, Coffignal, Pelle [LAD86] for elastoplastic materials. The present work is based on the Z^2 error estimator which has been proposed by Zienkiewicz and Zhu [ZIE87] and which is based on averaging techniques. It was applied to forming processes [ZIE88]. From numerical tests, we have shown in reference [FOU94] that the Orkisz' smoothing method improves the reliability of the estimation with respect to the standard global least square method. A Δ estimator is also proposed, which enables us to take into account the fact that the smoothed stress tensor does not verify the equilibrium equations. For both estimators, the studied examples show that the error due to the estimation (the relative difference between the exact error and the estimated error) is less than 20%.

At first, adaptive meshing techniques were based on the cutting up of elements into several pieces where the error indication is greater than a critical value. Refined and unrefined elements are then connected together [LÖH85]. This technique is used for the adaptive h hierarchical refinement method [ADE89]. Meanwhile, the most current approach is based on the rebuilding of a new mesh which satisfies a given size criterion on the whole domain. For non-steady forming processes, the time domain evolution makes the rebuilding inevitable. The frontal mesh generators are well adapted to this kind of problem [PER87]. On the other hand, any mesh generator can be transformed into an adaptive mesh generator, using a virtual

mapping of the real space. Mavripilis [MAV88] applied it to a Delaunay type mesh generator. Another approach is to introduce a quadtree structure into a Delaunay mesh generator and to modify it in order to take into account the size criterion [CHE88]. In the present work, adaptivity is introduced into the Delaunay remeshing procedure which have been suggested by Coupez and Chenot [COU92]. It is based on the two step following strategy : first generate a simple geometric mesh and then improve it in order to satisfy the size criterion.

In the second section, equations of the viscoplasticity problem are introduced and the Z^2 and Δ error estimators are described. The third section is dedicated to the adaptive remeshing algorithm itself along with its validations. In the fourth section, the efficiency of both error indicators are compared and the effect of a singularity in a viscoplasticity problem is studied. Finally, in the fifth section, the adaptive remeshing procedure is applied to error control for several forming processes.

2. Basic equations

2.1. Incompressible viscoplastic problem

The material is assumed to be homogeneous, isotropic and incompressible [1] and to obey the Norton-Hoff constitutive law [2],

$$\operatorname{div} \mathbf{v} = \operatorname{tr} \dot{\boldsymbol{\varepsilon}} = 0 \quad \text{on } \Omega \quad [1]$$

$$\mathbf{s} = \mu(\dot{\boldsymbol{\varepsilon}}) \dot{\boldsymbol{\varepsilon}} = 2 K (\sqrt{3} \dot{\boldsymbol{\varepsilon}})^{m-1} \dot{\boldsymbol{\varepsilon}} \quad [2]$$

with :

$$\mathbf{s} = \boldsymbol{\sigma} - \frac{1}{3} \operatorname{tr} \boldsymbol{\sigma} \mathbf{1} \quad [3]$$

$$\dot{\boldsymbol{\varepsilon}} = \sqrt{\frac{2}{3} \dot{\boldsymbol{\varepsilon}} : \dot{\boldsymbol{\varepsilon}}} \quad [4]$$

where \mathbf{v} is the velocity field on Ω , $\dot{\boldsymbol{\varepsilon}}$ is the strain rate tensor, \mathbf{s} is the deviatoric part of $\boldsymbol{\sigma}$, $\mathbf{1}$ is the unit tensor. μ is the viscosity of the material, K its consistency and m its strain rate sensitivity.

The friction between the tools and the workpiece Ω (see figure 1) is assumed to follow a power law which can be expressed in 2D as,

$$\boldsymbol{\tau} = -\alpha K |\Delta \mathbf{v}_t|^{q-1} \Delta \mathbf{v}_t \quad [5]$$

with :

$$\boldsymbol{\tau} = (\boldsymbol{\sigma} \mathbf{n}) \cdot \mathbf{t} \quad [6]$$

$$\Delta \mathbf{v}_t = (\mathbf{v} - \mathbf{v}_d) \cdot \mathbf{t} \quad [7]$$

where \mathbf{t} is the tangent to the tool surface, \mathbf{v}_d is the die velocity which is imposed, α and q are the friction coefficients.

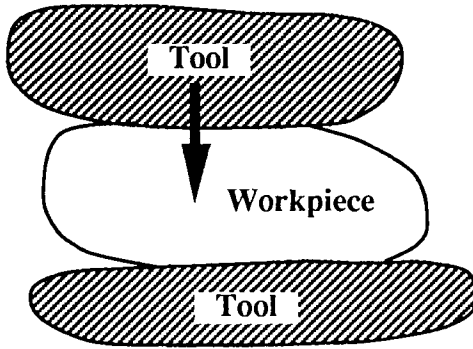


Figure 1. Workpiece and tools.

The equilibrium equations are given by [8-9], after neglecting inertia and gravity terms. The unilateral contact condition of the material with respect to the rigid dies is given by equation [10],

$$\operatorname{div} \sigma = 0 \quad \text{on } \Omega \quad [8]$$

$$T = \sigma n = 0 \quad \text{on } \partial_T \Omega \quad [9]$$

$$(v - v_d) \cdot n \leq 0 \quad \text{on } \partial_d \Omega \quad [10]$$

where $\partial \Omega$ is the surface of Ω , $\partial_T \Omega$ is the free surface of Ω , $\partial_d \Omega$ is the part of $\partial \Omega$ in contact with a die.

The integral equation of the problem [ZIE 84] along with a penalty method for the incompressibility constraint [1] is written [11], for any virtual velocity field v^* which verifies [12],

$$\int_{\Omega} s : \dot{\epsilon}^* dw - \int_{\partial_d \Omega} \tau \cdot v^* ds + \rho \int_{\Omega} \operatorname{div} v \operatorname{div} v^* dw = 0 \quad [11]$$

$$v^* \cdot n = 0 \quad \text{on } \partial_d \Omega \quad [12]$$

where ρ is a large numerical coefficient. Six-noded quadratic isoparametric elements are used for the finite element space discretization [13] and a two points reduced integration rule is introduced for the evaluation of the penalty terms of [11]. A very simple one-level explicit Euler scheme [14] is used for the time discretization [BOH85],

$$x_h = \sum_k \hat{x}^k N_k ; \quad v_h = \sum_k \hat{v}^k N_k \quad [13]$$

$$\hat{x}_{t+\Delta t}^k = \hat{x}_t^k + \Delta t \hat{v}_t^k, \quad \text{for any node } k \quad [14]$$

where \hat{x}^k and \hat{v}^k are the nodal parameters of the coordinates and velocities interpolations, N_k are the interpolation functions, \hat{x}_t^k and \hat{v}_t^k are the values of the parameters at time t .

2.2. Error estimators

The discretization error is defined for the energy norm,

$$\|v - v_h\|_E = \left(\int_{\Omega} \mu^{-1}(s) (s - s_h) : (s - s_h) dw \right)^{\frac{1}{2}} \quad [15]$$

with :
$$\mu^{-1}(s) = \frac{1}{\mu(\dot{\epsilon})} \quad [16]$$

where s is the exact deviatoric stress tensor and s_h is the finite element stress tensor.

The Z^2 estimator only requires the calculation of \tilde{s}_h , a continuous deviatoric stress tensor close to s_h . According to results given in reference [FOU94], the Orkisz' smoothing method [LIS80] is used (see appendix for more details). The Z^2 estimator is written,

$$\theta^{Z^2} = \left(\int_{\Omega} \mu^{-1}(s_h) (\tilde{s}_h - s_h) : (\tilde{s}_h - s_h) dw \right)^{\frac{1}{2}} \quad [17]$$

As \tilde{s}_h does not verify the equilibrium equations [8-9], a correction Δs_h has been introduced into the Z^2 estimator and gives the following Δ estimator,

$$\theta^{\Delta} = \left(\int_{\Omega} \mu^{-1}(s_h) \left((\tilde{s}_h - s_h) : (\tilde{s}_h - s_h) + \Delta s_h : \Delta s_h \right) dw \right)^{\frac{1}{2}} \quad [18]$$

Δs_h is defined according to equation [19],

$$\Delta s_h = \frac{\partial s_h}{\partial v_h}(v_h) \Delta v_h \quad \text{on } \Omega \quad [19]$$

and verifies the integral form of the equilibrium equations [20-22],

$$\text{div} (\tilde{s}_h + \Delta s_h) = 0 \quad \text{on } \Omega \quad [20]$$

$$(\tilde{s}_h + \Delta s_h) n = 0 \quad \text{on } \partial_T \Omega \quad [21]$$

$$\left(\left(\tilde{s}_h + \Delta s_h \right) n \right) \cdot t = \tau(v_h + \Delta v_h) \quad \text{on } \partial_d \Omega \quad [22]$$

where $\tau(v)$ is defined by equation [5] and Δv_h is a kinetically admissible velocity correction which verifies [12].

Both estimators provide error indicators θ_e for each element e of the mesh, according to [23],

$$\theta = \left(\sum_e^{Nbelt} \theta_e^2 \right)^{\frac{1}{2}} \quad [23]$$

where $Nbelt$ is the total number of elements of the mesh. Assuming that the finite element method has a uniform convergence rate p on the whole domain, the optimal size h_e^{opt} of each element is expressed by,

$$h_e^{opt} = \left(\theta^{tol} \right)^{\frac{1}{p}} \left(\sum_e^{Nbelt} \left(\theta_e \right)^{\frac{2}{p+1}} \right)^{-\frac{1}{2p}} \left(\theta_e \right)^{\frac{-1}{p+1}} h_e \quad [24]$$

where θ^{tol} is the tolerated value of the error and h_e is the current size of the element. The optimal number of elements of the new mesh is then given by,

$$Nbelt^{opt} = \sum_e^{Nbelt} \left(\frac{h_e}{h_e^{opt}} \right)^2 \quad [25]$$

3. Adaptive remeshing technique

Depending on the severity of the deformations which are undergone by the workpiece during the process, it turns out that it is difficult to evaluate the complexity of the meshes to be constructed, as well as the required number of elements for a given accuracy. Subsequently, the remeshing technique must be particularly robust. Due to this, we have chosen a two step strategy : first geometric remeshing and then adaptive remeshing. During the first step, the size criterion is not really taken into account, but a coarse mesh is built with a minimal number of nodes. This way the finite element calculation is made possible and the mesh verifies the geometrical constraints of the problem. Indeed, if there is not enough memory space available in order to built an adapted mesh, it is still possible to continue the calculations. During the second remeshing step, the mesh is refined by the addition of internal nodes until the size criterion is verified.

3.1. Geometric remeshing

This remeshing algorithm is based on the Delaunay's tessellation method and on the creation of an initial outline of the mesh :

i/ Creation of the outline of the mesh

As the current boundary of the mesh is made of quadratic segments, it is first overdiscretized with linear segments, by addition of either a fixed or variable (for the adaptive strategy) number of nodes on each of the quadratic segments. Then the new boundary nodes which are located inside the tool surface are projected onto this surface (see figure 2.). These points give the outline of the domain to be meshed.

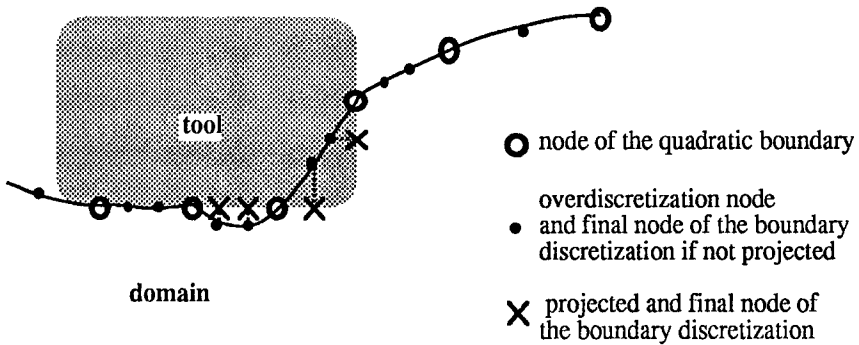


Figure 2. Creation of the outline of the mesh

iii/ Construction of the discretized boundary

From the outline of the mesh, we want to build a discretized boundary which has a minimal number of segments and which abides by the outline for a given accuracy. An iterative algorithm is used. Starting from the nodes of the outline, it eliminates all useless nodes which are not required to ensure the accuracy of the description of the domain and to ensure the validity of other criteria such as : maximal permitted size of segments, maximal length ratio between two connected segments and maximal curvature of a quadratic segment. The curvature of a linear segment [26] is defined as follows :

$$C_{\text{geo}} = \frac{a}{h} \quad [26]$$

where (a) is the chord (a) of the quadratic segment, based on the linear segment, which minimizes the difference of shape between the quadratic curve and the original outline (see figure 3.) ; (h) is the maximum distance between chord and arc of the quadratic segment. These first two steps are the most important ones in the geometric remeshing algorithm.

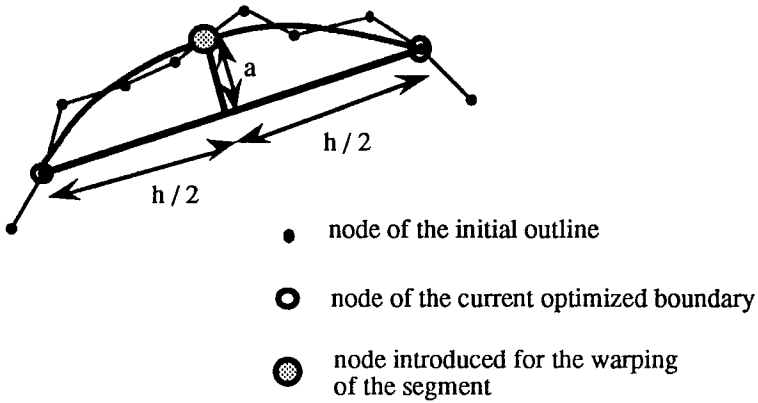


Figure 3. Curvature of a segment.

iii/ Tessellation without internal nodes

Delaunay's algorithm is used to create an initial tessellation with linear triangles, starting from the set of points of the discretized boundary. The steps are classical : creation of an initial fictitious triangle which contains the set of points, adding the points one by one in the tessellation, elimination of the nodes of the fictitious triangle, elimination of the triangles which are external to the outline.

iv/ Internal node addition

Internal nodes are added in order to improve the quality of the triangles. A weight is assigned to each node of the tessellation. It represents an average size of lines connected to the node. For boundary nodes, the weight is equal to the average length of the segments which are connected to it. This makes it possible to assign a weight to each triangle of the mesh, h^{ave} (the geometric average of the weights of its nodes) and to compare it with the actual characteristic length of the triangle, h^{act} (the square root of its surface). A node is then added inside the element for which the ratio h^{act} over h^{ave} is worse and not satisfactory. This node is put in the weighted centroid of the triangle. This paradoxical weighting (the node is put next to large triangles) accelerates the saturation of the node addition criterion and gives a better distribution of the nodes. The weight of the new node is the arithmetic average of the weights of the triangle multiplied by a refinement factor which is greater than 1 (for the adaptive strategy, this coefficient is set to 1.3 ; it permits us to reduce the number of nodes of the initial geometric mesh). Finally, the Delaunay's algorithm is used to insert the node in the tessellation.

vi/ Mesh improvement

The mesh quality is improved using two complementary iterative procedures : mesh regularization and topology improvement. During the regularization procedure, internal nodes are displaced to the weighted centroid of surrounding nodes (see figure 4.). The weights [27] depend on the quality of the triangles which is defined by the ratio between d^{ins} , the diameter of the inscribed circle and d^{enc} , the diameter of the encircling circle,

$$w_e = \frac{1}{1+W_{geo}} \quad \text{where :} \quad W_{geo} = \frac{d^{ins}}{d^{enc}} \quad [27]$$

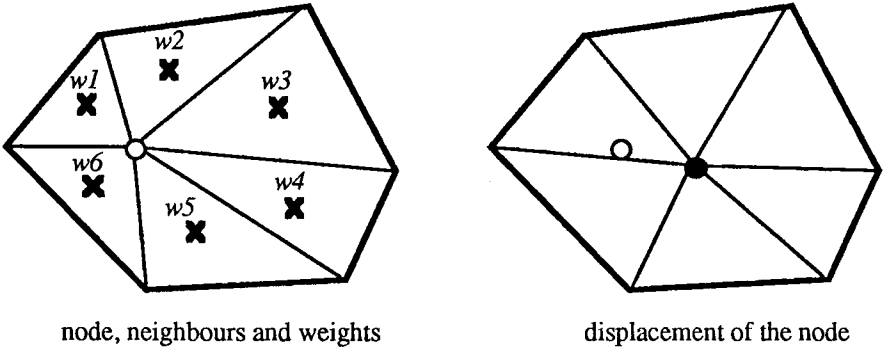


Figure 4. Geometrical mesh regularization.

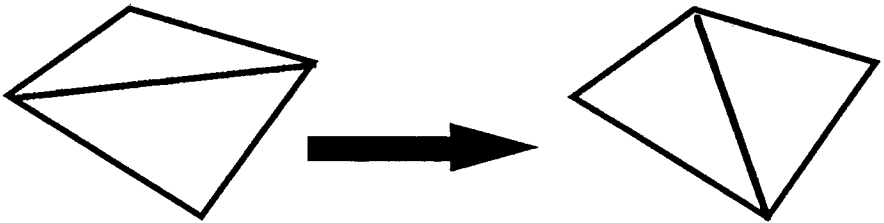


Figure 5. Topological mesh improvement.

vii/ Creation of six noded elements

Without adaptive remeshing, geometric remeshing operations end with the transformation of linear triangles into quadratic triangles : a node is added in the middle of each side of the mesh. For boundary segments, the warping procedure described in figure 3 is used.

3.2 Adaptive remeshing

First, h_e^{opt} , the size criterion which is calculated for each element of the initial mesh (father mesh) has to be enforced during the first two remeshing operations (i/ and ii/) of the creation of the discrete boundary. The size of a quadratic triangle is defined by the length of the longest side of the linear triangle (see figure 6.),

$$h = \underset{i=0}{\overset{2}{\text{Max}}} d(M_{2i+1} , M_{2i+3}) \tag{28}$$

where d is the distance between points.

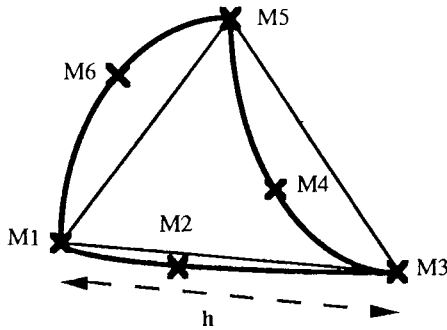


Figure 6. Size of a triangle.

During step i/ which gives the initial discretization of the new boundary, overd discretization nodes are added until the length of the sides is smaller than h^{opt} . During step ii/ this condition has to be preserved. The definition of the curvature is then modified during the iterative algorithm,

$$C_{mod} = C_{geo} + C_{fic} \tag{29}$$

$$C_{fic} = C_{max} \text{Hs} \left(\frac{h^{cur}}{h^{opt}} - 1 \right) \tag{30}$$

where h^{cur} is the current length of the segment, C_{max} is the maximal permitted value of the curvature and Hs is a smoothed Heaviside function (which is equal to 0 for negative values and equal to 1 for positive values).

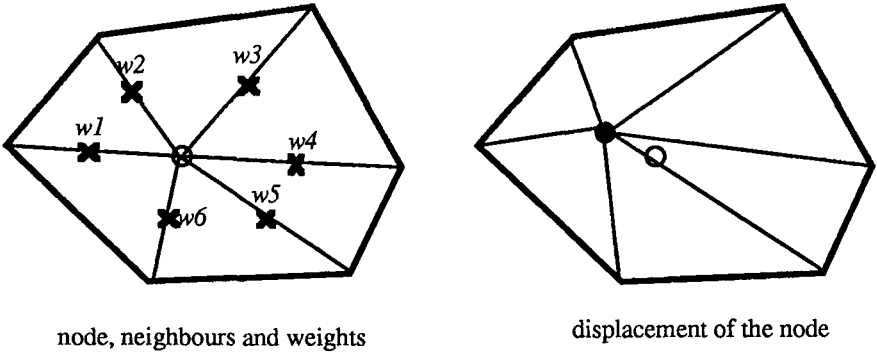


Figure 7. Adaptive mesh regularization.

Steps iii/ to v/ are kept unchanged. From step vi/, a search procedure is frequently used to find the element of the father mesh which contains a current point of the domain ; the h^{opt} value of this element is then assigned to the point. The algorithm is based on the inverse mapping of the shape functions of quadratic elements. It is speeded up by making a preliminary sorting out of applicant triangles.

vi/ Adaptive internal node addition

The procedure is like iv/ although the criterion of addition is based on the ratio h^{act} (actual size of the triangle which is defined according to equation [28]) over h^{opt} (which is interpolated at the centre of the triangle). Nodes are added until all triangles verify the adaptivity criterion.

vii/ Adaptive mesh improvement

The procedure is like v/, but the regularization operation takes into account the adaptivity criterion. Each internal node is then moved to the weighted centroid of the mid points of the sides which are connected to it (see figure 7). Weights are defined as follows,

$$w_e = \frac{1 + W_{ada}}{1 + W_{geo}} \quad [30]$$

$$W_{ada} = \frac{1}{2} Hs \left(\frac{h^{cur}}{h^{opt}} - 1 \right) \quad [31]$$

where H_s is another smoothed Heaviside function, h^{cur} is the length of the side, h^{opt} is the optimal length of the side and W_{geo} which is defined by equation [27] is always less than 0.5.

viii/ *Creation of six noded elements*

This step is quite similar to the vi/ step of the geometric mesh generator.

3.3 Numerical tests

At the end of remeshing operations, the optimal size criterion is verified for all the triangles. Therefore, the optimality of the mesh can be evaluated by the comparison between the number of created elements and the optimal number as given by equation [25]. The numerical results are summarized in figure 8 and the constructed meshes are shown in figure 9. Elasticity problems have been studied first (results a/, b/, c/). The results show a very good agreement between the optimal and the effective values, when the number of degrees of freedom is important, this is to say when the elements size is only defined by the adaptivity criterion and is no longer dependant on the geometry of the domain. For viscoplasticity problems (results d/, e/), the agreement is not so good. Two reasons can be invoked : first the geometries are more complex for forming processes and meshes are relatively coarser for non-linear problems ; second the variations of the values of h^{opt} are greater than the variations of elements size which are possible for a reasonable quality of the tessellation. So in this case, equation [25] does not permit us to estimate the optimal number of elements.

	Optimal number of elements	Number of elements created
Plate with a hole in the center	a/ 51	70
	b/ 820	828
Loaded hook	c/ 151	188
Indentation of a beam	d/ 58	105
	e/ 359	489

Figure 8. Efficiency of the adaptive mesh generator.

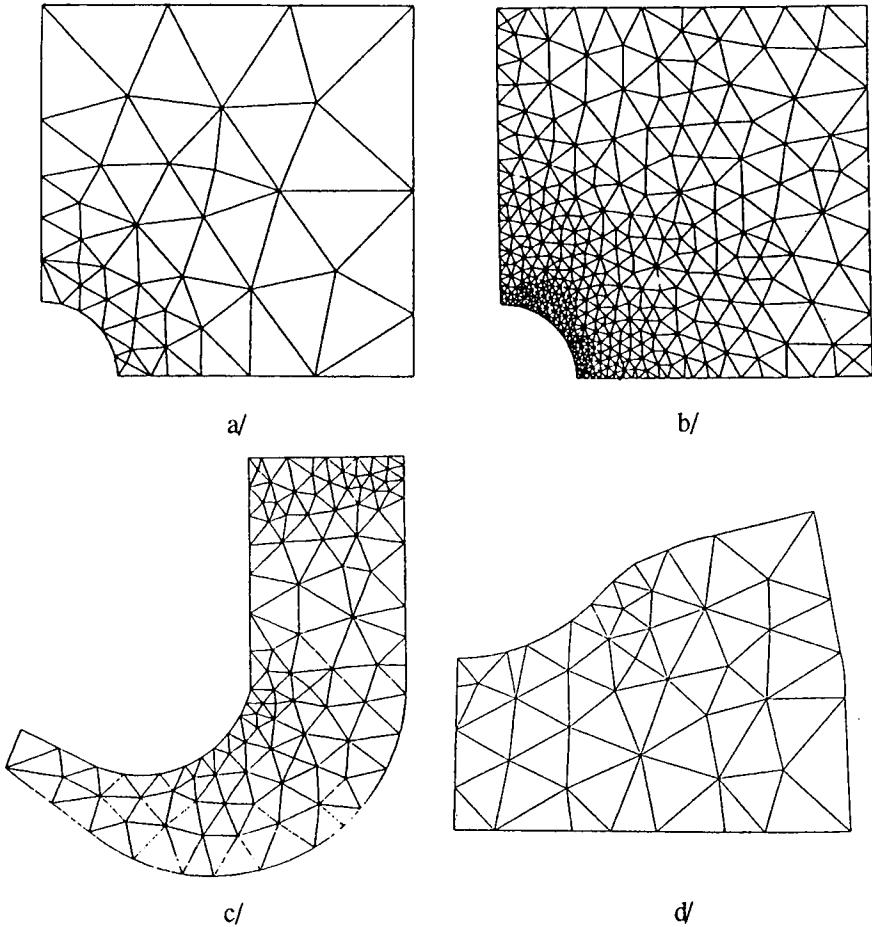


Figure 9. Some meshes constructed by the adaptive mesh generator.

4. Applications of the automatic remeshing procedure for steady state problems

Although we use quadratic elements, numerical experiments show that the convergence rate, p of the finite element method in the energy norm is close to 1. It is partly due to the two point reduced integration rule for the penalty terms of the integral formulation [12], and it is essentially due to the non linearities of the material behavior. However, when p is taken equal to 1 for the calculation of the element size [24], numerical experiments show that the number of created triangles is too large with respect to the required accuracy. On the other hand and in agreement with [ZIE88], a value of p equal to 2 allows for more optimal meshes. We can

invoke the great variations of the h^{opt} values for non linear flows, which are smoothed by taking p equal to 2. This is confirmed by the following examples for which p is equal to 2.

4.1. Comparison of error indicators

In reference [FOU94], we have shown that both Z^2 and Δ error estimators give comparable estimates, so we can compare the efficiency of the $\theta_e^{Z^2}$ and θ_e^Δ error indicators. The interrupted indentation of a beam using a rounded punch (see figure 10) under the plane strain assumption is considered.

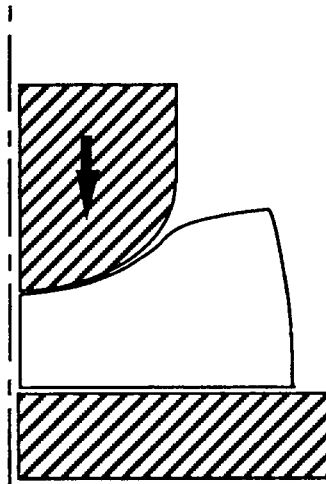


Figure 10. Interrupted indentation process.

The material data are as follows: $m = 0.15$, $q = 0.15$, $\alpha = 0.3 \text{ s}^{p-m} \text{ mm}^{-p}$. Both adaptive remeshing strategies are used ($\theta_e^{Z^2}$ and θ_e^Δ error indicators) for the two meshes of figure 11. The relative error is respectively evaluated to 10.6% and 6.1% from comparison with the finite element solution calculated on a much finer mesh. Adapted meshes are generated for respectively 10%, 6%, 3% and 5%, 4%, 3% of tolerated error. Z^2 and Δ error indicators are used successively along with the Orkisz' smoothing method. Results are summarized in figure 12. They show that the new meshes have the required estimated accuracy (the gap between the estimated error and the tolerated error is about 10%). Meshes which are obtained with the Δ indicator, are much finer (see figure 13 for example) and then the procedure is much more costly. So, although Z^2 and Δ estimators show nearly the same efficiency, the Z^2 adaptive remeshing strategy seems more efficient.

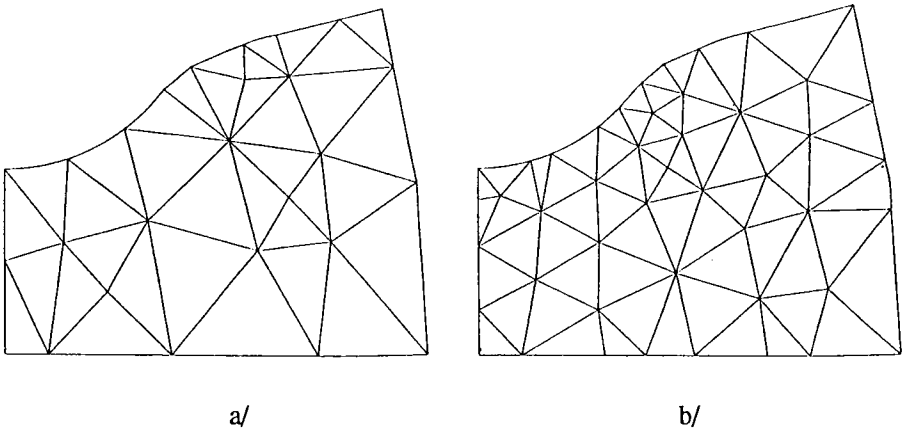
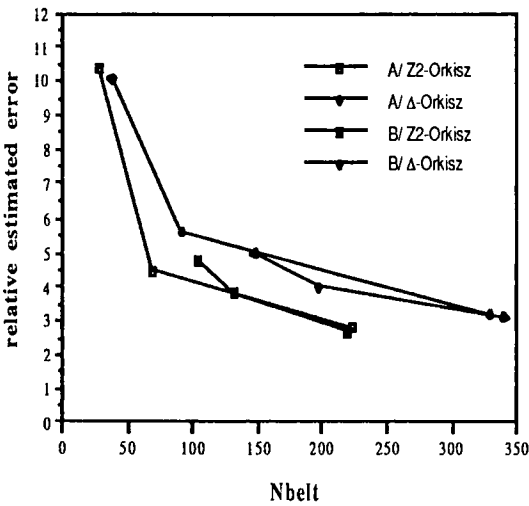


Figure 11. Meshes with 10.6% (a) and 6.1% (b) of calculated error for the tests of error indicators.



Comparison of adaptive remeshing strategies

Figure 12. Estimated error versus the number of elements of the mesh for both Z² and Δ adaptive remeshing strategies.

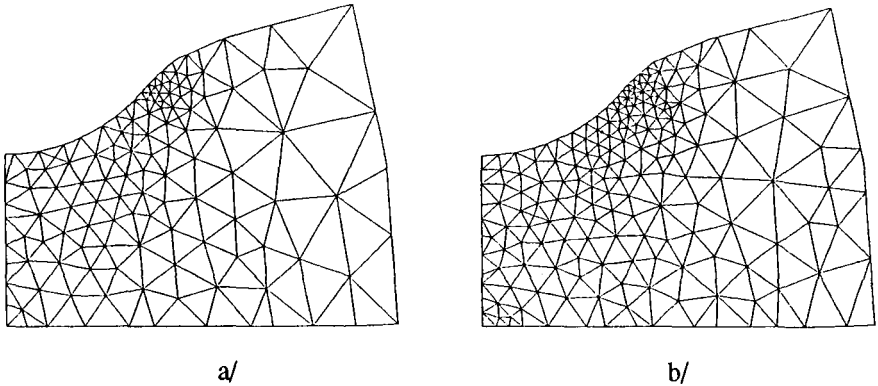


Figure 13. Meshes of 3% of tolerated error obtained from the 6.1% mesh (Figure 11b) along with the Z^2 (a) and the Δ (b) adaptive remeshing strategies.

4.2. Singular problems

During the calculation of the optimal mesh sizes [24], we have assumed that the finite element convergence rate, p is uniform. This hypothesis is not verified for a singular problem. Locally, the convergence rate is much less than p . Meanwhile, Szabo and Babuska [SZA91] mentioned that, according to numerical experiments, the convergence rate of an adaptive finite element method is asymptotically equal to p , even for a singular problem.

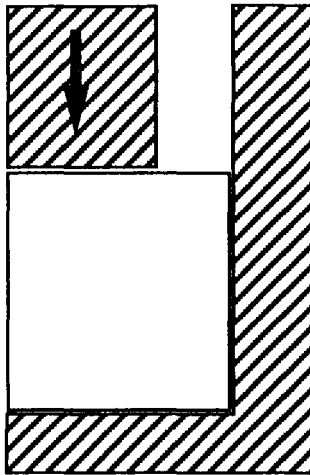


Figure 14. Singular backward extrusion problem.

Rivara [RIV86] has numerically shown this and has also shown that the efficiency of the error estimator is not decreased. Subsequently, Zienkiewicz and Huang [ZIE90] have suggested making several iterations of the adaptive remeshing procedure. According to this, we study a singular backward extrusion of a beam under the plane strain assumption (see figure 14). The punch angle is a singular point in the viscoplastic flow. The material data are similar for the indentation problem.

With the Z^2 estimator, the error is estimated to 17.5% on the initial mesh (see figure 15). The tolerated error is set to 5%. Four iterations are enough to reach the prescribed accuracy (see meshes of figure 15) : 13.8% (8.8% required), 7.8% (6.9% required) and 4.7% (5% required). The convergence rate of the adaptive finite element method is shown in figure 16, both for this problem and for the interrupted indentation problem of the previous paragraph (initial mesh of 6.1% of error) : they are quite the same.

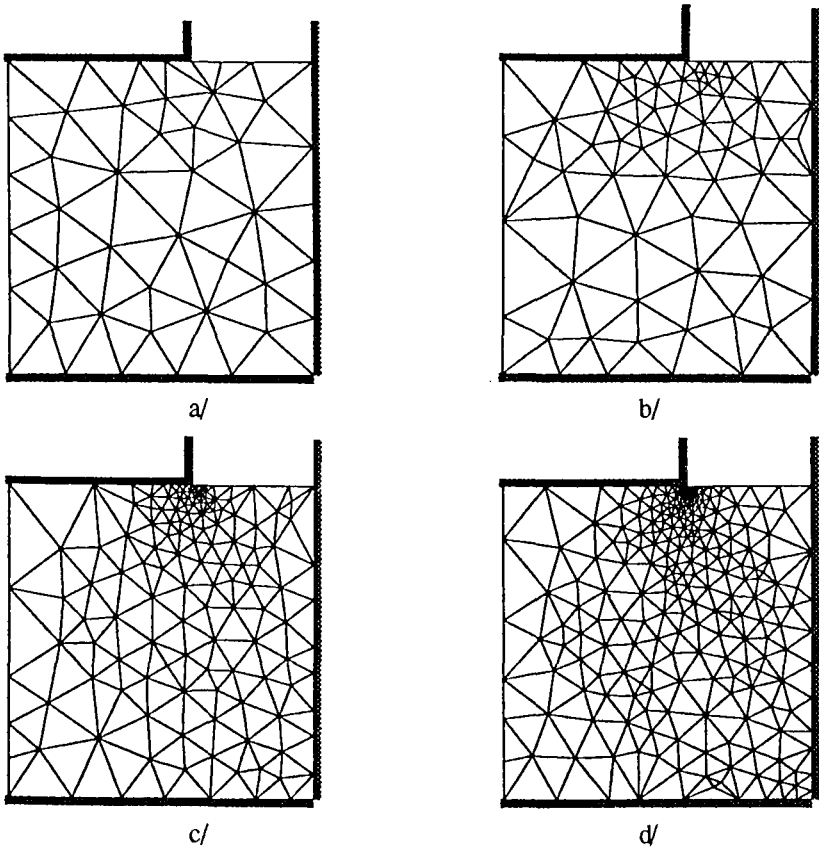
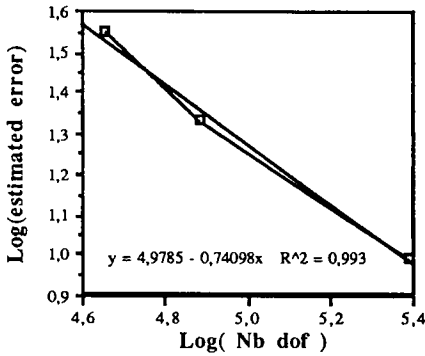
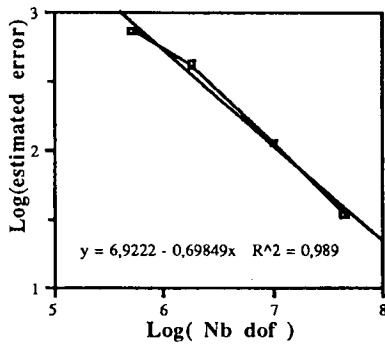


Figure 15. Singular backward extrusion problem :
 (a) initial mesh with 17.5% of error, (b) second mesh with 13.8% of error,
 (c) third mesh with 7.8% of error, (d) last mesh with 4.7% of error.



Convergence rate for the interrupted indentation problem

a/



Convergence rate for the backward extrusion problem

b/

Figure 16. Convergence rate of the adaptive finite element method for :
(a) the interrupted indentation problem starting from the 6.1% error mesh
(b) the singular backward extrusion problem (in base 2 logarithm).

5. Error control for metal forming processes

5.1. Error control

The non-steady state process is solved incrementally in time according to [14]. Therefore, the spatial discretization error is estimated at each time step, t . On the other hand, the time discretization error due to [14] is neglected. If the estimated

value is greater than the tolerated value, θ^{tol} a new mesh is generated which is adapted to the problem at time t . Notice that the remeshing operation can also be set off for reasons of a geometric type, such as : degeneracy of an element or of a boundary segment, penetration of the mesh in the tools because of a locally ill-adapted discretization, on a large value of the curvature of a segment of the free boundary. The computational time for the generation of a new mesh is generally low. It is less than the computational time of one increment of the process. Actually, there is an additional cost from the error control, but it is caused for two reasons : first the Newton-Raphson algorithm (which is used to solve equation [11]) has a lower rate of convergence after a remeshing operation (because the initial guess of the velocity field is not as good after remeshing), second , and it is the most essential reason, the time stepping has to be reduced because of the reduction of the size of the elements on the boundary of the domain (the duration of an increment of time has to be limited in order that no element of the free boundary be updated, according to [14] inside the tools).

The following examples have been studied in the framework of the plane strain assumption. We have used the Z^2 error estimator and the Orkisz' smoothing method. Moreover, we can define a measure of the error of the non-steady state process,

$$e_{\text{total}} = \left(\int_{\Omega} \int_0^{T_{\text{total}}} \mu^{-1}(s) (s - s_h) : (s - s_h) dt dw \right)^{\frac{1}{2}} \quad [32]$$

where T_{total} is the total duration of the process. e_{total} is estimated according to,

$$\theta_{\text{total}}^{Z^2} = \left(\sum_t (\theta^{Z^2}(t))^2 \right)^{\frac{1}{2}} \quad [33]$$

$\theta_{\text{total}}^{Z^2}$ is the total estimated error and $\theta^{Z^2}(t)$ is the current estimated error. Relative error values are calculated, introducing the following denominators for $\theta_{\text{total}}^{Z^2}$ and $\theta_{\text{total}}^{Z^2}$ respectively :

$$\|v_h\|_E = \left(\int_{\Omega} \mu^{-1}(s_h) s_h : s_h dw \right)^{\frac{1}{2}} \quad [34]$$

$$\|v_h\|_W = \left(\sum_t (\|v_h\|_E(t))^2 \right)^{\frac{1}{2}} \quad [35]$$

5.2. Indentation of a bar

We study the hot indentation of a viscoplastic bar (see figure 17). In this case, the material data are as follows : $m = 0.15$, $q = 0.15$, $\alpha = 1.3 \text{ s}^{\text{p}-\text{m}} \text{ m}^{-\text{p}}$. 16 remeshings are required in order to take into account the deformation of the bar and to maintain the estimated error under the tolerated value of 8% (see figure 18).

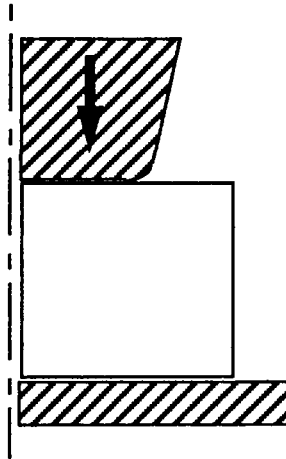
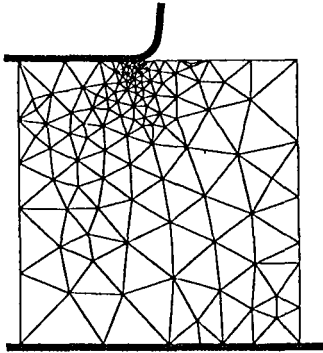
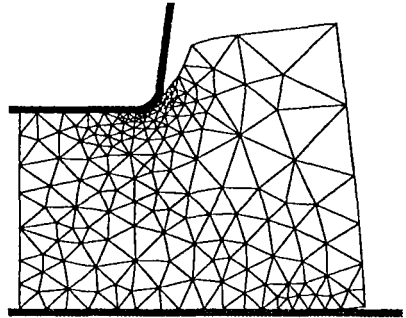


Figure 17. Indentation of a viscoplastic beam under the plane strain hypothesis.

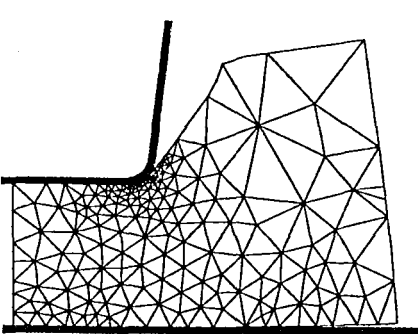
The evolution of the relative estimated error during the process is depicted in figure 19 and shows the error control procedure : when the current estimated error exceeds the prescribed value, a new mesh is generated for which the error is lower than the prescribed value. We can notice that the relative estimated total error can diminish during the simulation, because we use the current time of the process in equation [34] instead of the total time. At the end of the process, the estimated total error is equal to 6.5%.



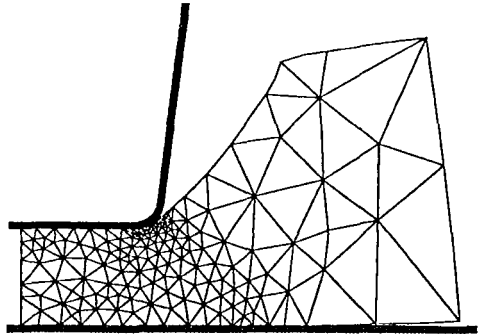
a/



b/



c/



d/

Figure 18. Adapted meshes for the indentation problem,
(for 0.5%, 31%, 50% and 66% of deformation)
with a tolerated value of error equal to 8%.

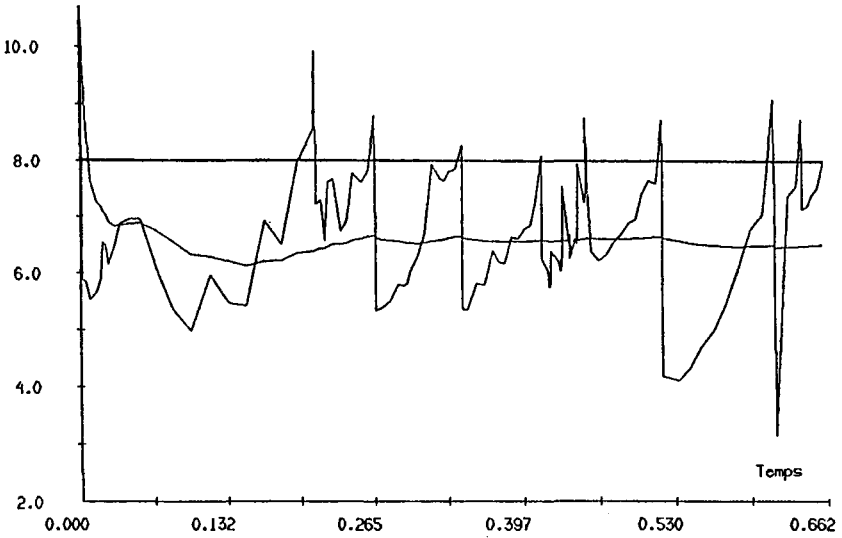


Figure 19. Evolution of estimated error during the indentation process : instantaneous error, total error and prescribed error.

5.3. Forging of a rib

An aeronautic rib is hot forged from a bar (see figure 20). The material data are the following : $m = 0.15$, $K = 9.7 \cdot 10^5 \text{ Pa s}^{-1} \text{ mm}^{-1}$, $q = 0.15$, $\alpha = 0.2 \text{ s}^{\text{P-m}} \text{ mm}^{-\text{P}}$.

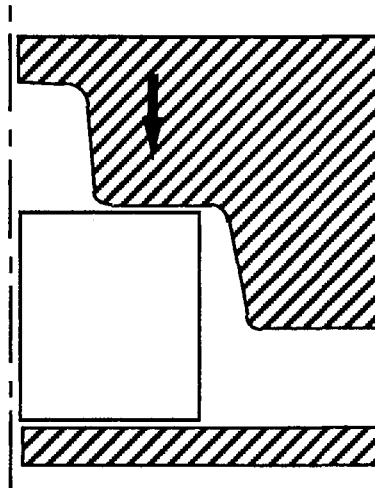


Figure 20. Forging of an aeronautical rib under the plane strain hypothesis.

The tolerated error is again set to 8%. 99 remeshing steps are required and the total error is estimated to be 6.2% at the end of the process. The evolution of the geometry of the domain being very important during the process, the refinement zones are much modified as can be seen in figure 21 (isovalues of optimal size maps at different times during the process).

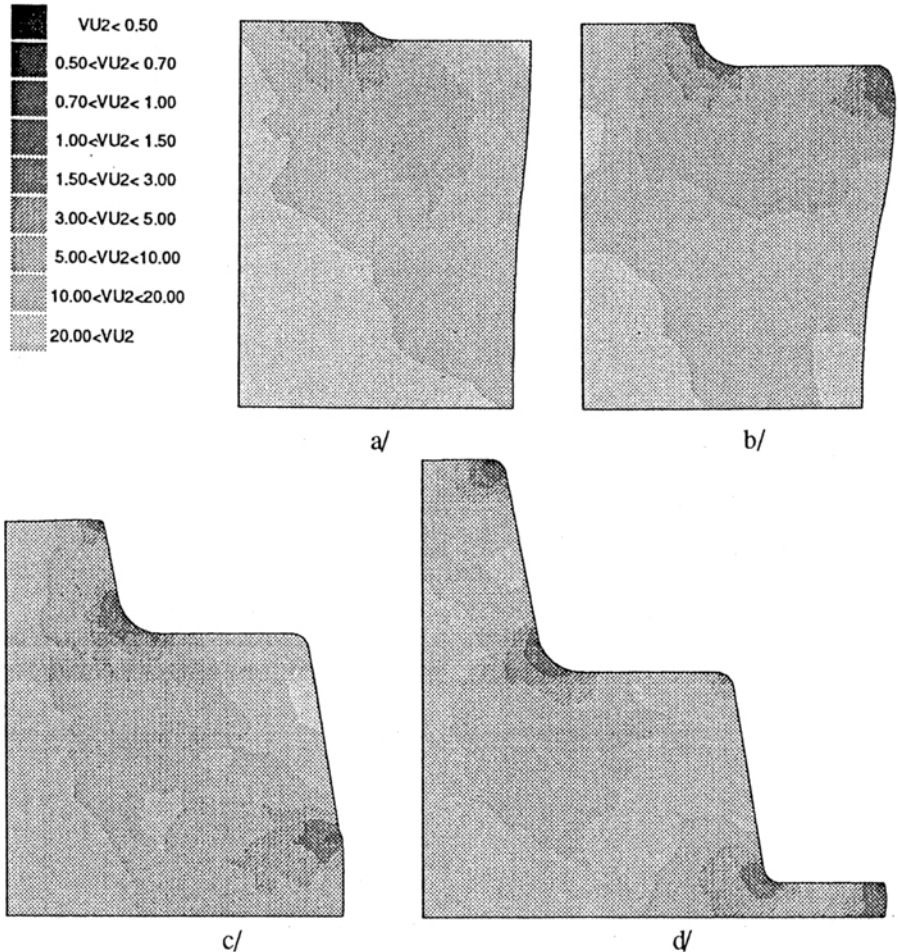


Figure 21. Isovalues of the optimal size of elements (for a/ 3.6%, b/ 10%, c/ 25% and d/ 35% of deformation) for the hot forging of a rib with 8% of tolerated error.

The numerous adaptive meshings make it possible to take into account the evolution of the problem (see figure 22) and the error control procedure is shown in figure 23. Sudden increases of error can appear during the simulation, because of sudden changes of the contact conditions.

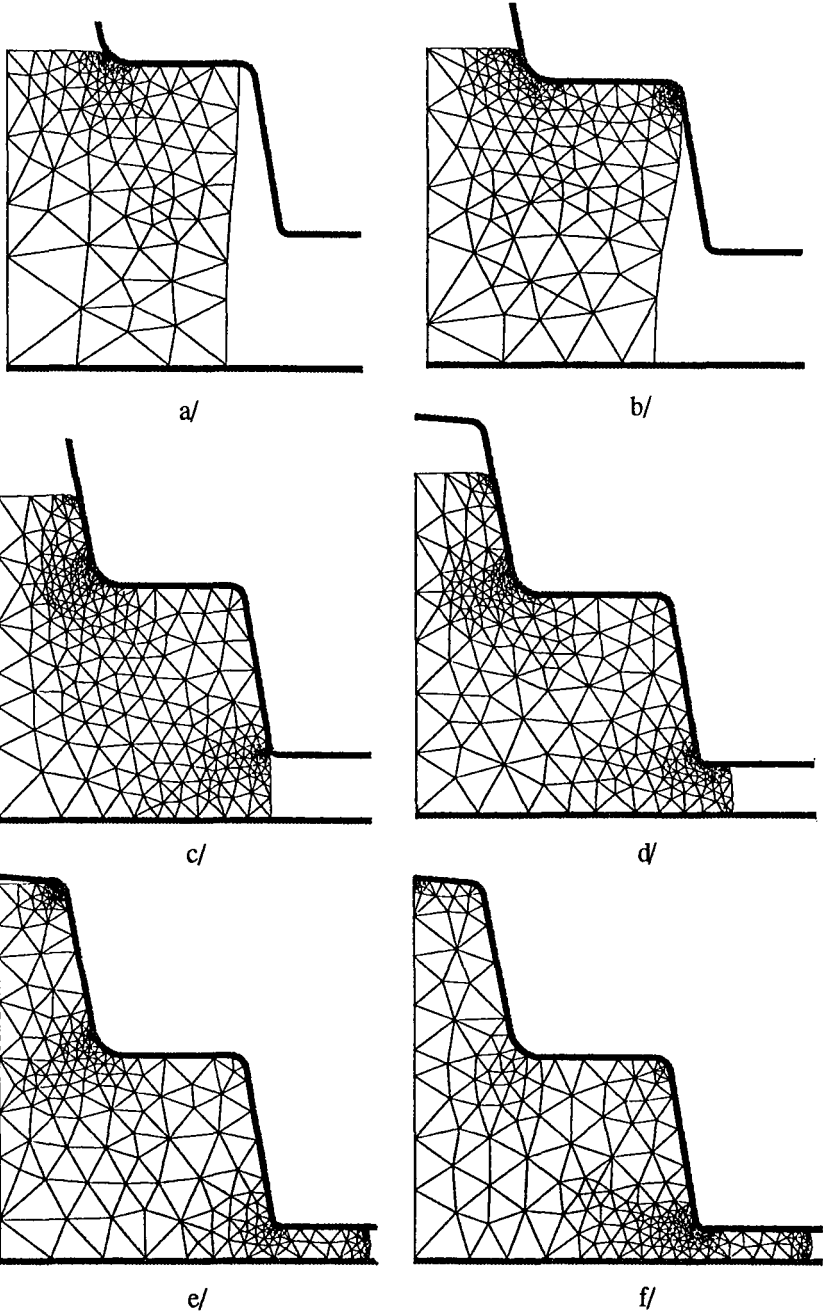


Figure 22. Adapted meshes for the hot forging of a rib for a/ 3.6%, b/ 10%, c/ 25%, d/ 30%, e/ 35% and f/ 36% of deformation.

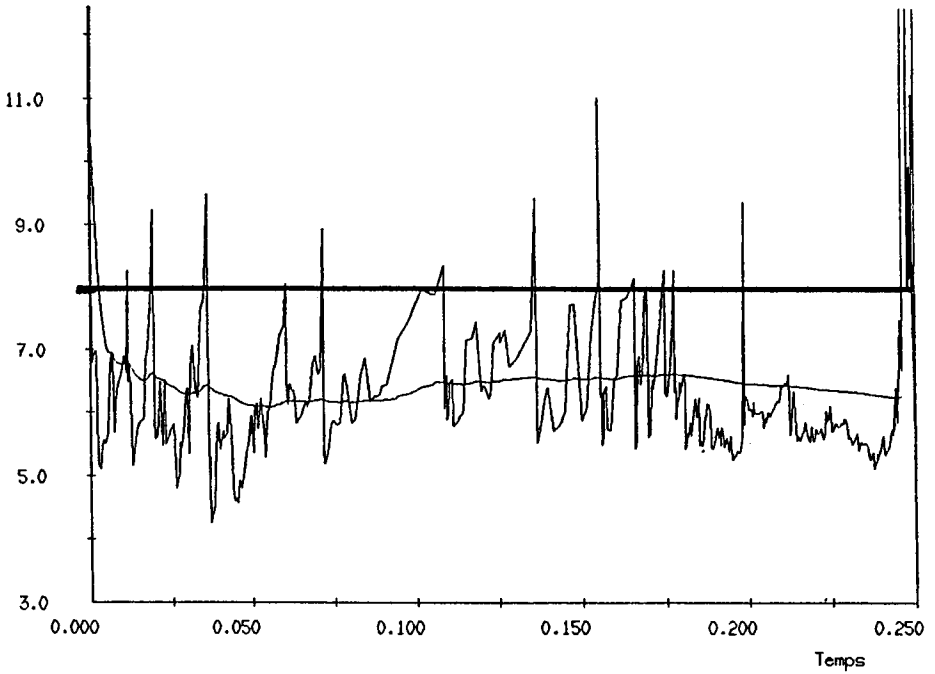


Figure 23. Evolution of estimated error during the hot forging of a rib : instantaneous error, total error and tolerated error.

5.4 Orthogonal metal cutting

Sekhon and Chenot [SEK93] have shown that a viscoplastic simulation code with thermo-mechanical coupling, can be used for the simulation of continuous chip formation during non-steady state orthogonal cutting (see figure 24).

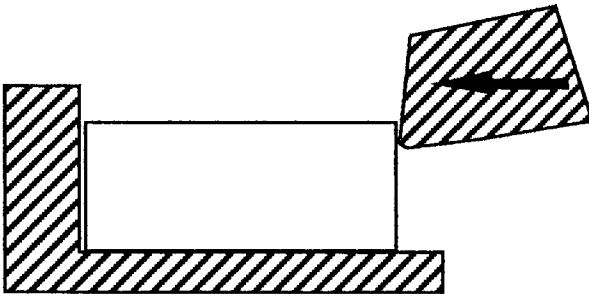
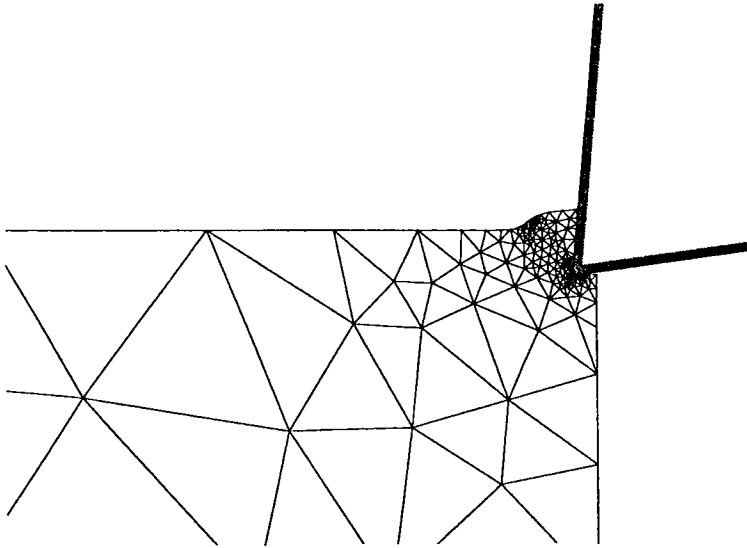
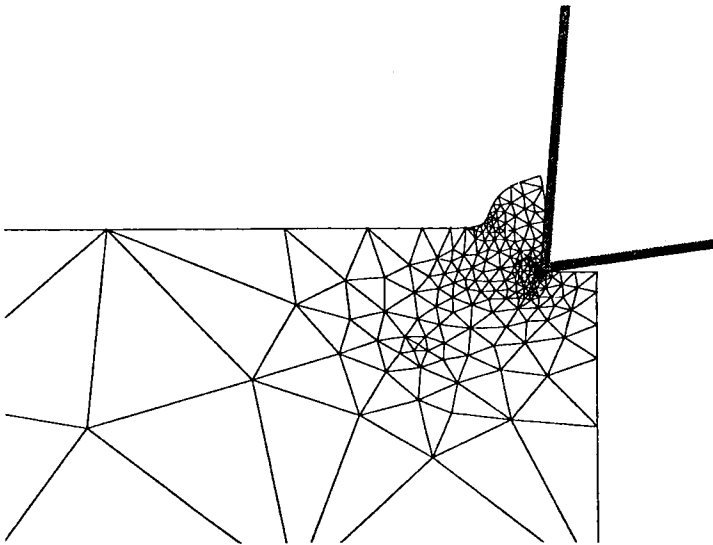


Figure 24. Non-steady state orthogonal metal cutting under the plane strain hypothesis.

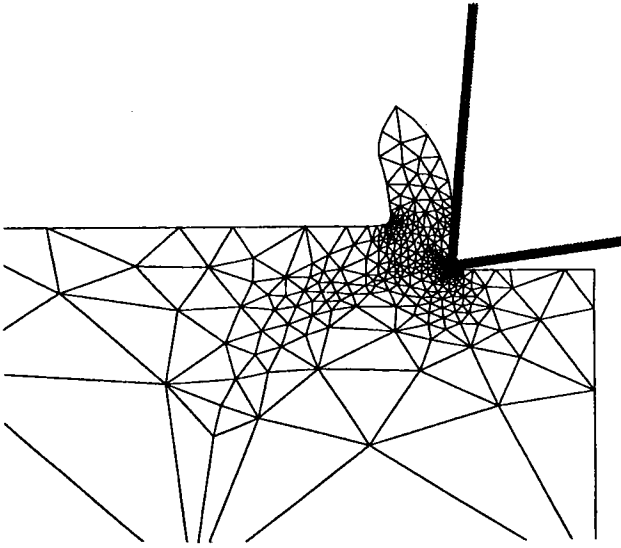


a/

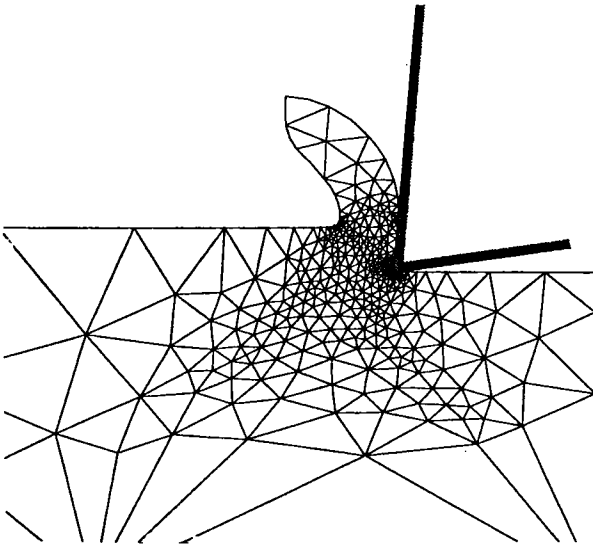


b/

Figure 25. Adapted meshes for the modelling of the formation of the chip during the orthogonal metal cutting process (a/ and b/)



c/



d/

Figure 25. Adapted meshes for the modelling of the formation of the chip during the orthogonal metal cutting process (c/ and d/)

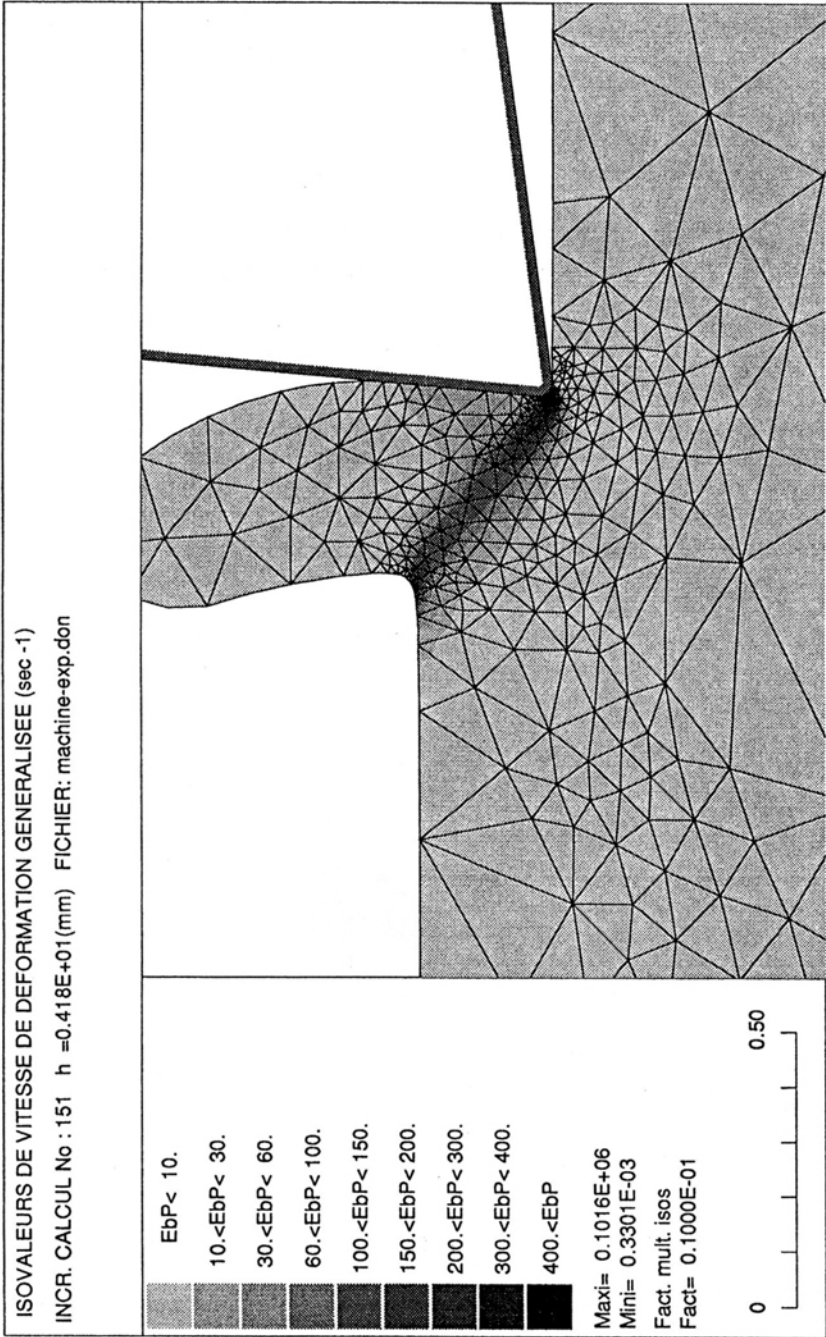


Figure 26. Isovalues of the equivalent strain rate at the end of formation of the chip.

The viscoplastic constitutive law includes strain hardening and temperature softening effects,

$$K = K_0 \left(1 + a \bar{\epsilon} \right) e^{\beta/T} \quad [36]$$

where $\bar{\epsilon}$ is the effective strain, T is the temperature of the material, K_0 , a and β are the parameters of the law. A description of the resolution of the thermal problem and of the thermo-mechanical coupling is given in reference [CES87]. The mechanical parameters of the material are the following : $m = 0.1$, $K = 1.25 \cdot 10^6 \text{ Pa s}^{-1} \text{ mm}^{-1}$, $q = 0.1$, $\alpha = 0.5 \text{ s}^{\text{D-m}} \text{ mm}^{-\text{D}}$, $a = 0.1$, $\beta = 200 \text{ K}^{-1}$.

The maximal tolerated error is set to 10%. 88 adaptive remeshings are required to study the formation of the chip and to reach a quasi-steady state. At this moment, the total error is estimated to 6.5%. Mesh evolution is given in figure 25. Adaptive remeshing makes it possible to keep very small elements near the cutting edge and to refine the meshes in the shear zone (see figure 26). In figure 27, the relative estimated error along with time is plotted both for the standard simulation (26% of estimated error at the end of the simulation) and for the error control procedure.

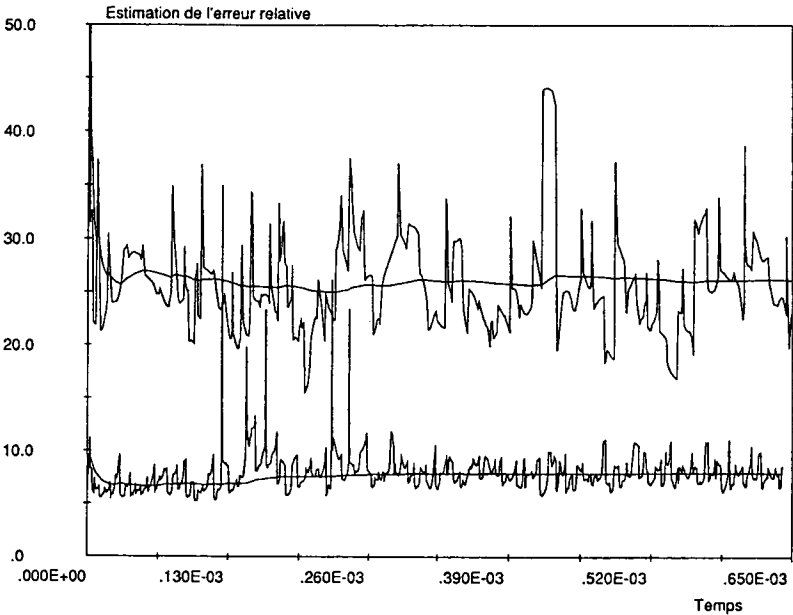


Figure 27. Evolution of estimated error during metal cutting. Above curves : standard remeshing strategy. Below curves : adaptive remeshing strategy.

6. Conclusion

The proposed adaptive remeshing procedure makes it possible to control the discretization error during the simulation of complex industrial forming problems which are non-linear and non-steady state in nature. It is based on a Delaunay type mesh generator. Robustness is established by the two step (geometric and adaptive) remeshing procedure and is confirmed by numerous automatic remeshing operations for complex geometries. Optimality of the tessellation is shown for smooth variations of the optimal size criterion, as is also found in elasticity problems. Reliability of the global remeshing procedure depends on many factors : the reliability of the Z^2 type error estimates for metal forming problems has been established in references [ZIE88,FOU94], and the reliability of the calculation of the mesh size criterion is shown by the good agreement between the tolerated value of error and the actual estimated error on the adapted mesh. Therefore, it makes it possible to control the discretization error for non-steady state processes. This is a first approach which should be improved on one hand by taking into account the other equations of the thermo-mechanical problem such as the thermal equations and the equations of the transfert of state variables after remeshing, and on the other hand, by defining error estimators for the global non-steady state problem which means taking into account the time discretization error.

References

- [ADE89] ADEJDJ G., AUBRY D., Development of a hierarchical and adaptive finite element software, *Comp. Meth. Appl. Mech. Eng.*, vol 75, 153-165, 1989
- [BAR89] BARANGER J., EL AMRI H., A posteriori error estimators for mixed finite element approximation of some quasi-newtonian flows, Invited lecture at the Workshop on innovative finite element methods, Rio de Janeiro, Nov. 27 to Dec 1st, 1989.
- [BOH85] BOHATIER C., CHENOT J.L., Finite element formulation for non steady-state visco-plastic deformation, *Int. J. Num. Meth. Eng. Comput.*, vol 5, 2-9, 1985.
- [CES87] CESCUTTI J.P., SOYRIS N., SURDON G., CHENOT J.L., Thermomechanical simulation finite element calculation of three-dimensional hot forging with remeshing, *Adv. Tech. Plasticity*, vol 2, 1051-1058, 1987.
- [CHE88] CHENG J.H., FINNIGAN P.M., HATHAWAY A.F., KELA A., SCHROEDER W.J., Quadtree/octree meshing with adaptive analysis, *Num. Grid Generation Comp. Fluid Mech.'88*, Pineridge Press, S. Sengupta, J. Haüser, P. R. Eiseman, J. F. Thompson editors, 633-642, 1988.
- [COU89] COUPEZ T., CHENOT J.L., A new approach for enforcing the incompressibility in the finite element viscoplastic flow formulation, *Computational Plasticity Models Softwares and Applications*, Owen, Hinton, Oñate editors, Pineridge Press, 615-626, 1989.
- [COU92] COUPEZ T., CHENOT J.L., Lage deformations and automatic remeshing, *Computational Plasticity*, Pineridge Press, D. R. J. Owen, E. Oñate, E. Hinton editors, 1077-1088, 1992
- [FOU94] FOURMENT L., CHENOT J.L., Error estimators for viscoplastic materials : application to forming processes, to appear ...
- [HAN92] HANS RAJ K., FOURMENT L., COUPEZ T., CHENOT J.L., Simulation of industrial forging of axisymmetrical parts, *Engineering Computations*, vol 9, 575-586, 1992

- [HET92] HETU J.F., PELLETIER D.H., Adaptive remeshing for viscous incompressible flows, *AIAA Journal*, vol 30, n°8, August 1992.
- [LAD86] LADEVEZE P., COFFIGNAL G., PELLE J.P., Accuracy of elastoplastic and dynamic analysis, Accuracy Estimates and Adaptivity for Finite Elements, ch 10, 181-203, J. Wiley, Chichester, 1986.
- [LIS80] LISZKA T., ORKISZ J., The finite difference method at arbitrary irregular grids and its application in applied mechanics, *Comp. and Struct.*, vol 11, 83-95, 1980.
- [LÖH85] LÖHNER R., MORGAN K., ZIENKIEWICZ O.C., An adaptive finite element procedure for compressible high speed flows, *Comp. Meth. Appl. Mech. Eng.*, vol 51, 441-465, 1985.
- [MAV88] MAVRIPILIS D.J., Adaptive mesh generation for viscous flows using Delaunay triangulation, *Num. Grid Generation Comp. Fluid Mech.'88*, Pineridge Press, Sengupta, Häuser, Eiseman, Thompson editors, 611-620, 1988.
- [PER87] PERAIRE J., VAHDATI M., MORGAN K., ZIENKIEWICZ O.C., Adaptive remeshing for compressible flow computations, *J. Comp. Phys.*, vol 72, 449-466, 1987.
- [RIV86] RIVARA M.C., Adaptive finite element refinement and fully irregular and conforming triangulations, *Accuracy Estimates and Adaptive Refinement in finite element Computations*, Babuska, Zienkiewicz, Gago, Oliveira editors, John Wiley & Sons, section 20, 1986.
- [SEK93] SEKHON G.S., CHENOT J.L., Numerical simulation of continuous chip formation during non-steady orthogonal cutting, *Engineering Computations*, vol 10, 31-48, 1993.
- [SZA91] SZABO B.A., BABUSKA I., Finite element analysis, John Wiley & Sons, 1991.
- [ZIE84] ZIENKIEWICZ O.C., Flow formulation for numerical solution of forming processes, *Numerical Analysis of Forming Processes*, Pittman et al. editors, Wiley, New York, 1-44, 1984.
- [ZIE87] ZIENKIEWICZ O.C., ZHU J.Z., A simple error estimator and adaptive procedures for practical engineering analysis, *Int. J. Num. Meth. Eng.*, vol 24, 337-357, 1987.
- [ZIE88] ZIENKIEWICZ O.C., LIU Y.C., HUANG G.C., Error estimation and adaptivity in flow formulation for forming problem, *Int. J. Numer. Methods Eng.*, vol 25, 23-42, 1988.
- [ZIE90] ZIENKIEWICZ O.C., HUANG G.C., A note on localization phenomena and finite element analysis in forming process, *Communication in Appl. Num. Meth.*, vol 6, 71-76, 1990.

Appendix : Orkisz' method

The Orkisz' method is a local finite difference smoothing technique which is a second order method for calculation of $\tilde{\epsilon}_h$. $\tilde{\epsilon}_h$ is interpolated with the same interpolation functions as the velocity field v_h :

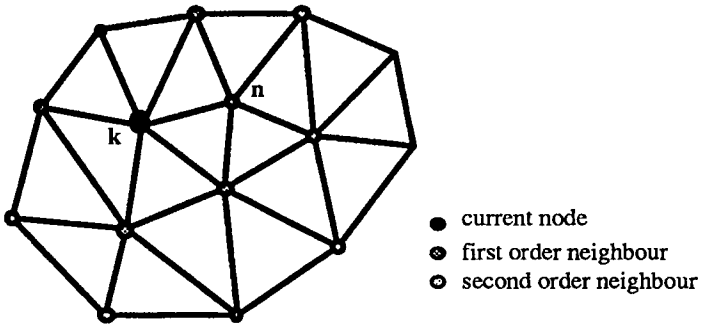
$$\tilde{\epsilon}_h = \sum_k \epsilon_h^{N_k} N_k$$

where $\hat{\epsilon}_h^k$ are the parameters of the interpolation. For any node k , $\hat{\epsilon}_h^k$ is computed from a second order Taylor series expansion of the velocity field at several neighbouring nodes, n of k :

$$\begin{aligned} \text{for } i= 1, 2 \quad v_i(n) &= v_i(k) + \sum_{j=1}^2 \frac{\partial v_i}{\partial x_j}(k) \Delta x_j(n) \\ &+ \frac{1}{2} \sum_{j=1}^2 \sum_{l=1}^2 \frac{\partial^2 v_i}{\partial x_j \partial x_l}(k) \Delta x_j(n) \Delta x_l(n) + O_i(\Delta r(n)^3) \end{aligned}$$

where : for $j= 1, 2$ $\Delta x_j(n) = x_j(n) - x_j(k)$

$$\Delta r(n) = \left(\sum_{j=1}^2 \Delta x_j(n)^2 \right)^{\frac{1}{2}}$$



Neighbouring nodes of node k

Therefore, the first and second order derivatives of the velocity field, $\frac{\partial v_i}{\partial x_j}(k)$ and $\frac{\partial^2 v_i}{\partial x_j \partial x_l}(k)$ minimize the following local least square functionals :

$$\text{for } i= 1, 2 \quad \Pi_i(k) = \sum_n \left(\frac{O_i(\Delta r(n)^3)}{\Delta r(n)^3} \right)^2$$

This problem is well defined for a sufficient number of neighbours. The calculation can be improved by introducing the incompressibility constraint, the free surface equation and the symmetry conditions :

$$\frac{\partial v_1}{\partial x_1} + \frac{\partial v_2}{\partial x_2} = 0$$

$$\frac{\partial v_1}{\partial x_1} \cdot n_1 + \frac{1}{2} \left(\frac{\partial v_1}{\partial x_2} + \frac{\partial v_2}{\partial x_1} \right) (n_2 - n_1) - \frac{\partial v_2}{\partial x_2} \cdot n_2 = 0$$

$$\frac{\partial v}{\partial t} \cdot n = \frac{\partial v}{\partial n} \cdot t = 0$$

$$\frac{\partial^2 v}{\partial t^2} \cdot n = \frac{\partial^2 v}{\partial t \partial n} \cdot t = \frac{\partial^2 v}{\partial n^2} \cdot n = 0$$

where (n_1, n_2) and (t_1, t_2) are the surface normal and tangent components.

These equations are taken into account via a penalty formulation. In general, 10 neighbours are selected allowing for the conditioning of the problem. Finally, \tilde{s}_h is interpolated like $\tilde{\varepsilon}_h$ and its nodal parameters are calculated from ε_h^k according to the constitutive equation.